

2002

Paleomagnetism and geochronology of the Ecstall pluton in the Coast Mountains of British Columbia: Evidence for local deformation rather than large-scale transport

Robert F. Butler
University of Portland, butler@up.edu

George E. Gehrels

Suzanne L. Baldwin

Cameron Davidson

Follow this and additional works at: http://pilotscholars.up.edu/env_facpubs

 Part of the [Geology Commons](#), [Geophysics and Seismology Commons](#), and the [Tectonics and Structure Commons](#)

Citation: Pilot Scholars Version (Modified MLA Style)

Butler, Robert F.; Gehrels, George E.; Baldwin, Suzanne L.; and Davidson, Cameron, "Paleomagnetism and geochronology of the Ecstall pluton in the Coast Mountains of British Columbia: Evidence for local deformation rather than large-scale transport" (2002). *Environmental Studies Faculty Publications and Presentations*. 33.
http://pilotscholars.up.edu/env_facpubs/33

This Journal Article is brought to you for free and open access by the Environmental Studies at Pilot Scholars. It has been accepted for inclusion in Environmental Studies Faculty Publications and Presentations by an authorized administrator of Pilot Scholars. For more information, please contact library@up.edu.

Paleomagnetism and geochronology of the Ecstall pluton in the Coast Mountains of British Columbia: Evidence for local deformation rather than large-scale transport

Robert F. Butler, George E. Gehrels, and Suzanne L. Baldwin¹

Department of Geosciences, University of Arizona, Tucson, Arizona, USA

Cameron Davidson

Department of Geology, Beloit College, Beloit, Wisconsin, USA

Received 16 August 2000; revised 27 April 2001; accepted 18 July 2001; published 18 January 2002

[1] Samples for geochronologic, geobarometric, and paleomagnetic analyses were collected across the northern portion of the Ecstall pluton southeast of Prince Rupert, British Columbia. Al-in-hornblende geobarometry indicates pressures from 740 ± 10 to 840 ± 30 MPa corresponding to crystallization depths of ~ 25 to ~ 30 km. U/Pb analyses of zircons from western, central, and eastern localities within the pluton yield crystallization ages of 91.5 ± 1.0 Ma, 90.8 ± 1.0 Ma, and 90.5 ± 1.0 Ma, respectively. Rock magnetic experiments, reflected light microscopy, and thermal demagnetization behavior suggest that natural remanent magnetism is carried by low-Ti titanohematite. Unblocking temperatures of the characteristic remanent magnetization (ChRM) are dominantly in the 560°C to 630°C range, with age of magnetization approximated by the $^{40}\text{Ar}/^{39}\text{Ar}$ hornblende ages of 84.2 ± 0.10 Ma on the western margin and 76.4 ± 0.6 Ma in the center of the pluton. Site-mean ChRM directions were isolated for paleomagnetic samples from 23 sites and are distributed along a small circle with subhorizontal axis at $\sim 340^\circ$ azimuth. ChRM directions from the central portion of the pluton are concordant with the expected Cretaceous magnetic field direction, while ChRM directions from the western margin are discordant by $>70^\circ$. Folding of the Ecstall pluton, either during Late Cretaceous west directed thrust transport above the convex upward Prince Rupert Shear Zone or during younger deformation of the pluton and underlying shear zone, can account for the paleomagnetic data and is consistent with the geochronologic, geobarometric, and structural geologic observations.

INDEX TERMS: 1525 Geomagnetism and Paleomagnetism: Paleomagnetism applied to tectonics (regional, global); 1527 Geomagnetism and Paleomagnetism: Paleomagnetism applied to geologic processes; 8105 Tectonophysics: Continental margins and sedimentary basins; 8110 Tectonophysics: Continental tectonics-general (0905);

KEYWORDS: Paleomagnetism, Cretaceous, British Columbia, Tectonics

1. Introduction

[2] Some of the first discordant paleomagnetic directions in Cretaceous rocks of the North American Cordillera were discovered by Symons [1974] in plutons near Prince Rupert, British Columbia. Discordant paleomagnetic directions were observed in the Late Cretaceous Ecstall and Butedale plutons and the mid-Cretaceous plutons of Stephens Island and Pitt Island (Figures 1 and 2). These Cretaceous plutons all have paleomagnetic directions with shallow inclinations and clockwise-rotated declinations when compared to expected Cretaceous directions. These discordant directions were initially interpreted to indicate northeast-side-up tilting of these plutonic rocks [Symons, 1977]. Later, when discordant paleomagnetic directions were found to be widespread within the North American Cordillera, the discordance was attributed to tectonic motion of crustal blocks involving ~ 3000 km of northward transport and clockwise vertical axis rotation [Beck, 1976, 1980; Beck *et al.*, 1981; Irving *et al.*, 1985, 1996]. North-

ward transport is interpreted to have occurred in the interval from 90 Ma to 50 Ma.

[3] Interpretation of discordant paleomagnetic directions from plutonic rocks is not straightforward because paleohorizontal at the time of magnetization can only be inferred indirectly. There are no direct lithologic recordings of paleohorizontal as with stratified rocks. As a result, a "tilt versus translation" controversy has ensued regarding the discordant paleomagnetic directions from plutonic rocks of the North Cascades and Coast Mountains batholith [Butler *et al.*, 1989; Brown and Burmester, 1991; Vandall, 1993; Ague and Brandon, 1996, 1997; Anderson, 1997].

[4] Discordant paleomagnetic directions have also been observed in Cretaceous sedimentary and volcanic rocks of the northern North American Cordillera [Wynne *et al.*, 1995; Ward *et al.*, 1997]. Some workers have concluded that the consistently shallow paleomagnetic inclinations confirm the transport interpretation of discordant paleomagnetic directions from the plutonic rocks. The tectonic transport interpretation has become known as the Baja British Columbia hypothesis [Umhoefer, 1987; Cowan, 1994; Cowan *et al.*, 1997]. This is because the implied mid-Cretaceous location of the Insular superterrane and at least the western portion of the Coast Mountains and North Cascades is in the position relative to North America now occupied by Baja California. However, concerns about compaction shallowing of paleomagnetic inclination in sedimentary rocks and about reli-

¹Now at Department of Earth Sciences, Syracuse University, Syracuse, New York, USA.

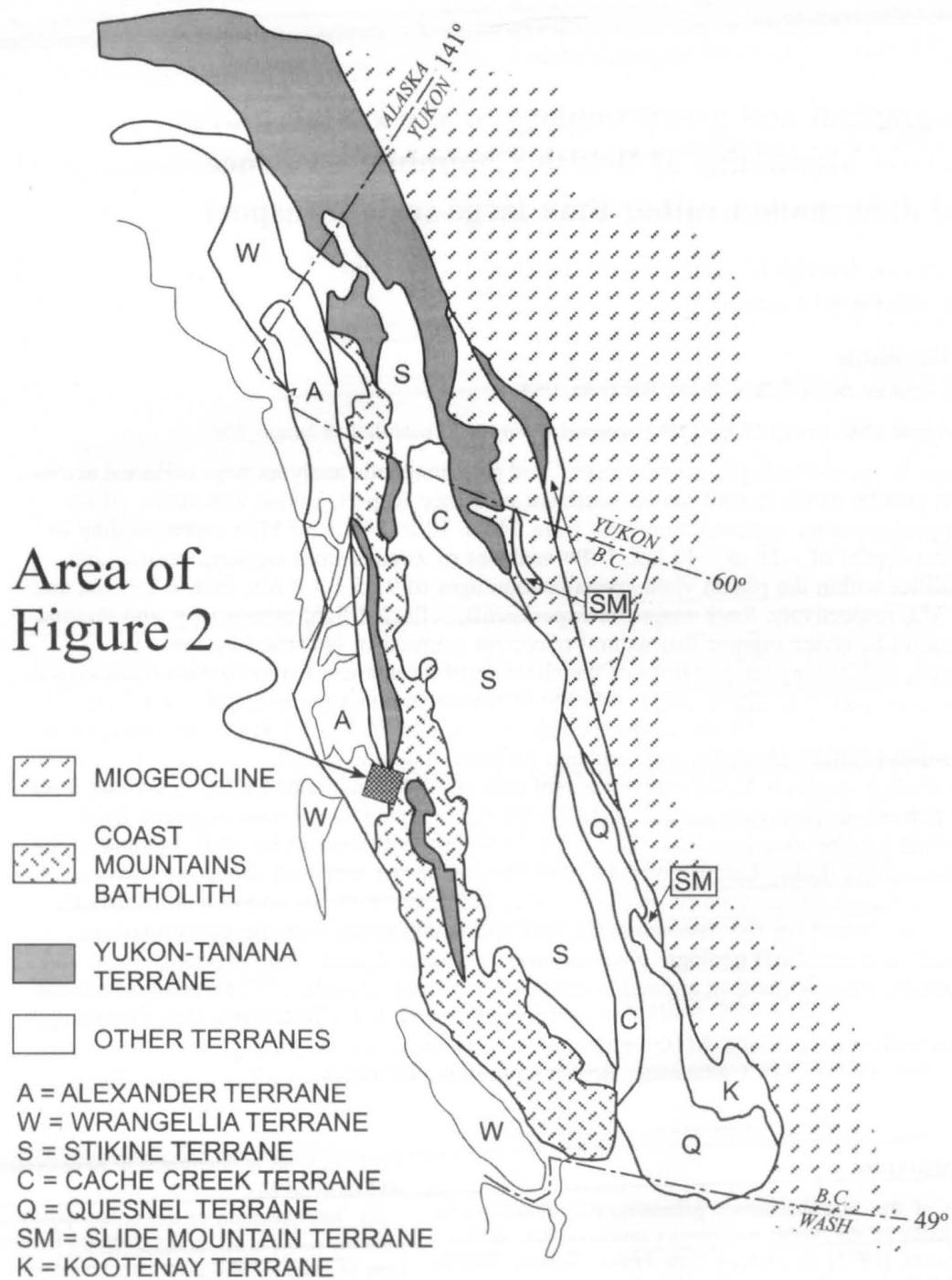


Figure 1. Generalized geological map of the Coast Mountains batholith and terranes of the northern Cordillera. Area shown in regional geologic map of Figure 2 is outlined. Adapted from *Gehrels and Kapp* [1998].

ability of paleomagnetic directions from the Cretaceous volcanic rocks have arisen. Indeed, the Baja British Columbia hypothesis remains controversial and has been the focus of a recent international conference [Mahoney *et al.*, 2000]. The importance of this paleogeographic model reaches beyond the North American Cordillera. Resolution of the controversy is important to understanding the tectonics of continental margins affected by compressional, transpressional, and strike-slip plate tectonic boundaries all of which have occurred along the western margin of North America during the past 100 m.y. [Hollister and Andronicos, 1997].

[5] Because the Baja British Columbia hypothesis depends critically on paleomagnetic observations from Cretaceous plutonic rocks of the North American Cordillera, it is important to examine

possibilities that local geological structures could be responsible for some of the discordant directions. Additional sampling and modern paleomagnetic analyses coupled with geochronologic and geologic observations may lead to refined understanding of the origin of the discordant directions. Our results reported here indicate that local folding of the Ecstall pluton in the Prince Rupert area can account for the discordant paleomagnetic directions without latitudinal transport >1000 km.

2. Geologic Setting

[6] The Ecstall pluton is a large granitic body that underlies much of the western flank of the Coast Mountains near Prince

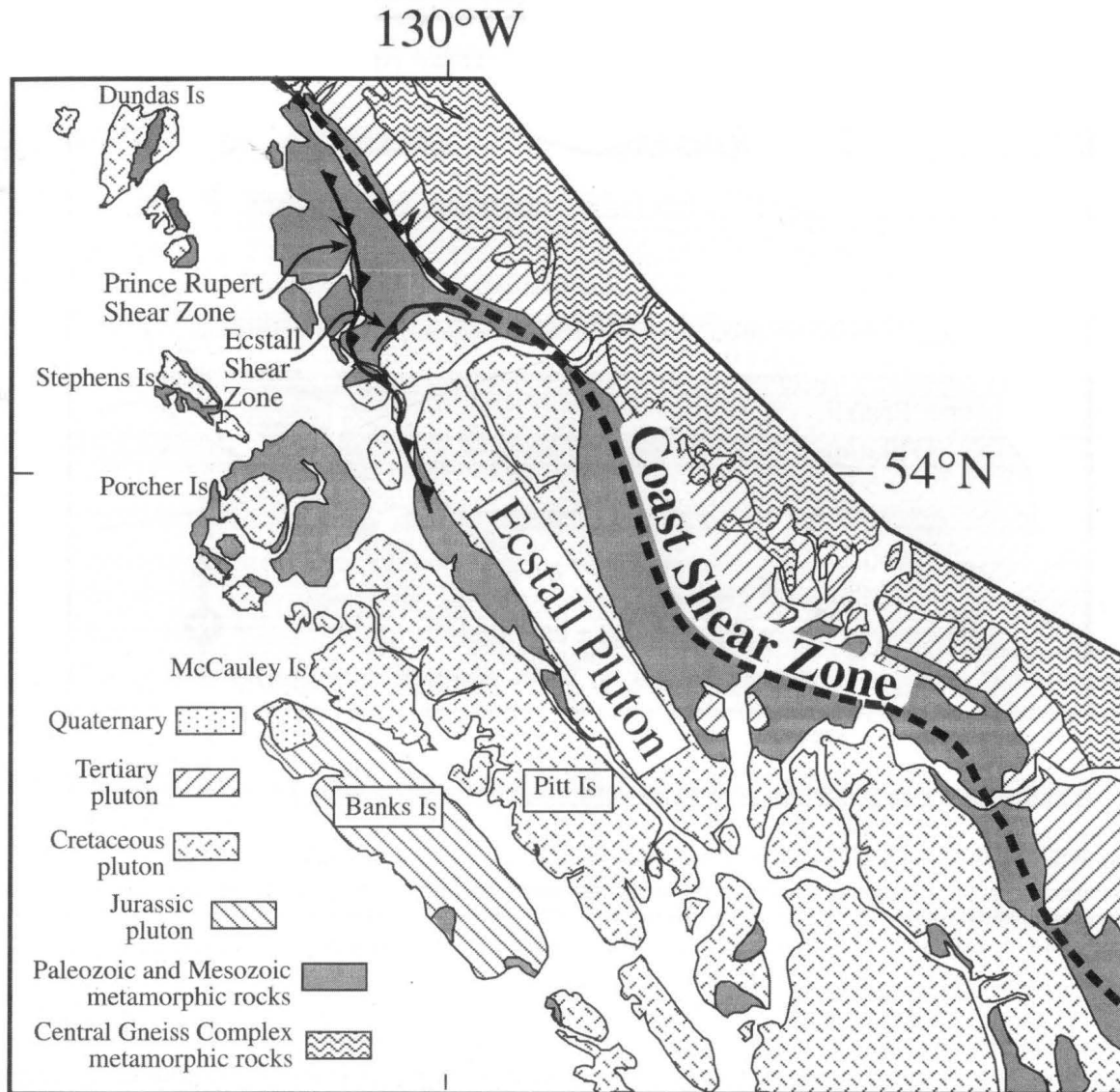


Figure 2. Geologic map of Prince Rupert region. Distribution of geologic units is from *Hutchison* [1982], while geologic structures are adapted from *Crawford and Hollister* [1982] and *Crawford et al.* [1987, 2000].

Rupert (Figure 2). It is elongate in shape, with a southwest-northeast width of 12–20 km and a northwest-southeast length of >80 km. Compositionally, the body is mainly hornblende quartz diorite and granodiorite, with subordinate diorite along its northeast margin [Hutchison, 1982]. The age of the body was reported to be 98 ± 4 Ma on the basis of two discordant U-Pb analyses of large zircon populations [Woodsworth et al., 1983]. As described below, new U-Pb analyses indicate that the crystallization age is ~ 90 Ma.

[7] The northern part of the body, where our study was conducted, was intruded into schist and gneiss derived from pelitic and psammitic marine strata with subordinate volcanic horizons [Hutchison, 1982]. The tectonic affinity of these country rocks is uncertain, with possibilities including the Alexander terrane [Armstrong and Runkle, 1979], the Yukon-Tanana terrane [Crawford et al., 2000], or the Gravina belt [Gehrels, 2001]. The Prince Rupert Shear Zone dips northeast at a moderate angle along the southwestern margin of the Ecstall pluton. The northward continuation of the shear zone steepens to nearly vertical. From regional patterns of metamorphic grade and dip of the Prince Rupert Shear Zone, it is inferred that this shear zone steepens with increasing depth in the crust. In the footwall of this thrust are Paleozoic rocks of the Alexander terrane overlain by Jura-Cretaceous strata of the Gravina

belt [Woodsworth et al., 1983; Crawford et al., 1987, 2000; Gehrels, 2001].

[8] The Ecstall pluton is known to have been emplaced at deep crustal levels on the basis of geobarometric data from both the pluton and its country rocks. Country rocks adjacent to the north end of the body are uniformly kyanite and staurolite bearing, recording depths of ~ 25 km during metamorphism related to emplacement [Crawford et al., 1987, 2000]. The presence of primary epidote in the pluton suggests that crystallization occurred at ~ 25 km depth [Crawford and Hollister, 1982; Zen and Hammerstrom, 1984]. As described below, Al-in-hornblende analyses of the Ecstall pluton document crystallization at lower crustal levels. K-Ar ages of ~ 87 Ma (hornblende) and ~ 70 Ma (biotite) [Armstrong and Runkle, 1979] and $^{40}\text{Ar}/^{39}\text{Ar}$ analyses presented below indicate that the pluton was cooled to $\sim 500^\circ\text{C}$ within 15 m.y. after emplacement.

3. Hornblende Geobarometry

[9] The Ecstall pluton is one of the classic localities used by Hammerstrom and Zen [1986] to calibrate the empirical Al-in-

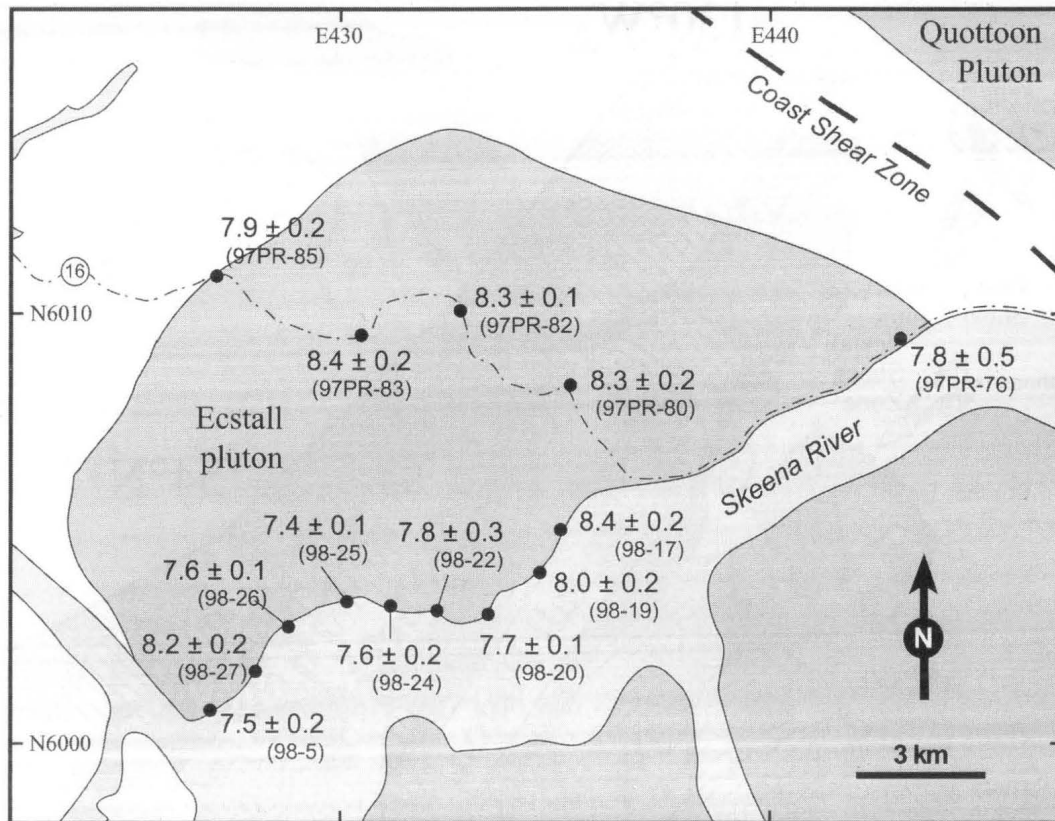


Figure 3. Geobarometric determinations from northwestern portion of the Ecstall pluton. Solid circles indicate locations of samples for which aluminum in hornblende barometric data were obtained. Sample numbers are in parentheses; compositions of samples are listed in Table A1 (electronic supplement); pressures are shown in kbar ($\pm 1\sigma$). Dash-dotted line is Yellowhead Highway (#16). Latitude and longitude grid is UTM coordinates (zone 9).

hornblende geobarometer. For this study, we measured the Al content of hornblende from 14 samples across the northern portion of the Ecstall pluton (Figure 3) to constrain the depth of crystallization. Hornblende chemistry was measured on the University of Wisconsin Cameca SX-50 electron microprobe using an accelerating voltage of 15 kV and beam current of 20 μ A. Following the classification scheme of Leake [1978], amphibole rims measured in this study range from magnesian hastingsitic hornblende to magnesian hastingsite (Table A1, electronic supplement¹). Mg/(Mg + Fe²⁺) ranges from 0.49 to 0.58, and Na + K ranges from 0.63 to 0.84. A minimum of 10, but typically 16 rim analyses were used to calculate the average pressure for a given sample (Table A1, electronic supplement).

[10] Pressures were calculated using the experimental calibration of Schmidt [1992]. Following Schmidt [1992], we normalized hornblende compositions based on Σ cations Ca-Na-K = 13 and then used charge balance to calculate Fe³⁺. Reported errors are standard deviation of the mean ($\pm 1\sigma$) and do not include analytical or calibration uncertainties. Schmidt [1992] quotes an uncertainty of ± 0.6 kbar for his calibration. Calculated pressures from this study range from 740 ± 10 to 830 ± 30 MPa (7.4 ± 0.1 to 8.4 ± 0.3 kbar; Figure 3). These pressures agree with pressure estimates based on phase equilibria in the surrounding metamorphic rocks [Crawford

and Hollister, 1982] and the pluton [Zen and Hammerstrom, 1984]. Implied depths of crystallization are in the 22–25 km range.

4. Geochronology

4.1. U/Pb Analyses

[11] For U/Pb age determinations, one sample was collected from each of three locations within the Ecstall pluton (Figure 4): (1) Ecstall East ($54^{\circ}13.505' N$, $129^{\circ}53.157' W$); (2) Ecstall Central ($54^{\circ}11.325' N$, $129^{\circ}59.873' W$); and (3) Ecstall West ($54^{\circ}9.411' N$, $130^{\circ}8.744' W$). Zircons were separated from the samples utilizing standard mineral separation techniques, and grains were separated into size fractions using disposable nylon sieve screens. Grains from a variety of size fractions were analyzed by conventional isotope dilution, thermal ionization mass spectrometry, as described by Gehrels [2000].

[12] The sample from the east side of the body (Ecstall East) yields five concordant analyses (Table A2, electronic supplement; Figure 5), with $^{206}\text{Pb}^*/^{238}\text{U}$ ages that range from 90.0 to 90.9 Ma. The interpreted crystallization age is 90.5 ± 1.0 Ma (95% confidence limits). The sample from the central part of the body (Ecstall Middle) yields four concordant analyses and a single grain that is highly discordant. The concordant analyses (shown on Figure 5) yield a crystallization age of 90.8 ± 1.0 Ma. The discordant grain apparently includes radiogenic components with an average age of ~ 700 Ma when projected from 90.8 Ma. The sample from the west side of the body (Ecstall West) yields four concordant analyses, with $^{206}\text{Pb}^*/^{238}\text{U}$ ages that range from 91.2 to 91.7 Ma (Table A2, electronic supplement; Figure 5). The interpreted crystallization age is 91.5 ± 1.0 Ma.

¹ Supporting data Tables A1, A2 and A3 are available via Web browser or via Anonymous FTP from <ftp://agu.org>, directory "apend" (Username = "anonymous", Password = "guest"); subdirectories in the ftp site are arranged by paper number. Information on searching and submitting electronic supplements is found at http://www.agu.org/pubs/esupp_about.html.

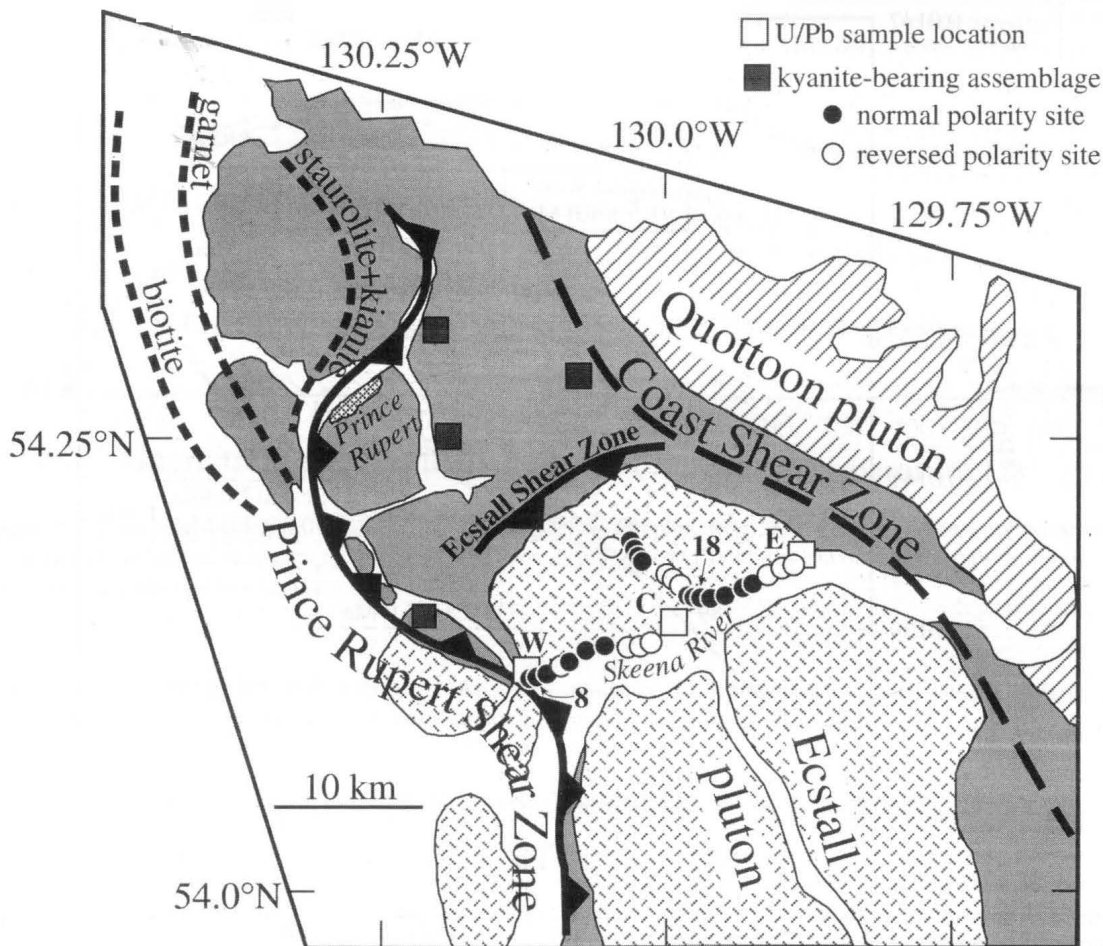


Figure 4. Locations of paleomagnetic and geochronologic sampling sites for Ecstall pluton. Metamorphic isograds and locations of kyanite-bearing assemblages were adapted from Crawford and Hollister [1982]. Locations of paleomagnetic sampling sites are indicated by solid circles for normal-polarity sites and open circles for reversed polarity sites. Sites labeled 8 and 18 are paleomagnetic sites ET008 and ET018, respectively, from which samples for $^{40}\text{Ar}/^{39}\text{Ar}$ geochronology were obtained. Squares labeled W, C, and E are locations of U/Pb samples from the western, central, and eastern parts of the Ecstall pluton.

[13] The U-Pb age data demonstrate that the Ecstall pluton was emplaced during a short interval of mid-Cretaceous time. Although the uncertainties of the three ages overlap at the 95% confidence level (largely due to systematic errors), the $^{206}\text{Pb}/^{238}\text{U}$ ages demonstrate that the body is composite and becomes slightly younger to the east.

4.2. The $^{40}\text{Ar}/^{39}\text{Ar}$ Analyses

[14] Samples for $^{40}\text{Ar}/^{39}\text{Ar}$ geochronology were obtained from the western margin (sample 8, Figure 4) and the central portion (sample 18, Figure 4) of the Ecstall pluton. Biotite and hornblende (>99% pure) were separated from quartz diorite using standard separation techniques. Mineral separates were wrapped individually in Sn foil, along with biotite standard GA1550 [McDougall and Harrison, 1999] used to monitor the neutron dose. Samples were vacuum sealed in quartz tubes and irradiated for 20 hours in position L-67 of the Ford Reactor at the University of Michigan.

[15] Argon analyses were performed in the Noble Gas Laboratory at the University of Arizona. Extraction of gas from the samples was accomplished using a double-vacuum, resistance-heated tantalum furnace with temperature control via a thermocouple in contact with the bottom of the crucible and mounted on the outer (low) vacuum side of the furnace. Three getters were used for purification of the extracted gas. Isotopic analyses were

performed using a VG5400 mass spectrometer with an ion-counting electron multiplier. Machine mass discrimination and sensitivity were determined from repeated analysis of atmospheric argon. Data reduction was completed on a PC using in-house programs. Samples were corrected for blanks, neutron-induced interfering isotopes, decay of ^{37}Ar and ^{39}Ar , mass discrimination, atmospheric argon, as well as H^{35}Cl , H^{36}Cl , and H^{37}Cl . Correction factors used to account for interfering nuclear reactions were determined by analyzing argon extracted from irradiated CaF_2 and K_2SO_4 and are $(^{36}\text{Ar}/^{37}\text{Ar})_{\text{Ca}} = 0.00027$, $(^{38}\text{Ar}/^{37}\text{Ar})_{\text{Ca}} = 0.00043$, $(^{39}\text{Ar}/^{37}\text{Ar})_{\text{Ca}} = 0.00105$, $(^{40}\text{Ar}/^{39}\text{Ar})_{\text{K}} = 0.017$, $(^{38}\text{Ar}/^{39}\text{Ar})_{\text{K}} = 0.012$. Isochron analysis indicated that the trapped argon in all samples was at, or near, atmospheric in composition. The $^{40}\text{Ar}/^{39}\text{Ar}$ step heating results are listed in Table A3 (electronic supplement) and age spectra are illustrated in Figure 6. All ages were calculated using the decay constants recommended by Steiger and Jager [1977]. Stated precision for $^{40}\text{Ar}/^{39}\text{Ar}$ ages includes all uncertainties in the measurement of isotope ratios and are quoted at the 1σ level. The errors do not include that associated with the J parameter which is <0.5%.

4.2.1. Sample 8. [16] Thin section observations of sample 8 provide evidence for alteration including sericitization of plagioclase and reaction rims on biotite. The preservation of igneous textures and lack of fabric development suggest that the rocks were statically altered. The $^{40}\text{Ar}/^{39}\text{Ar}$ step heat experiments on

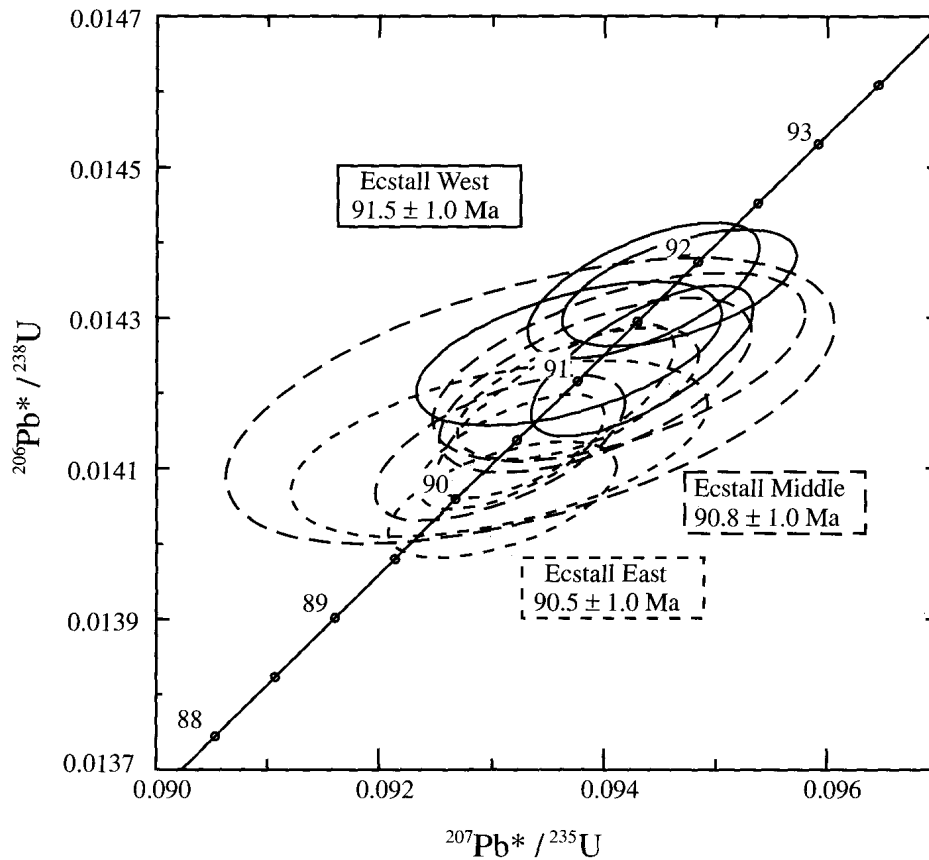


Figure 5. U-Pb concordia diagrams for zircon grains separated from three samples of the Ecstall pluton. Concordia plots were produced using the programs of Ludwig [1991a, 1991b]. Ellipses are 95% confidence limits.

amphiboles from sample 8 from the western side of the Ecstall pluton (Figure 4) yielded a complex age spectrum with apparent ages ranging from ~60 to 85 Ma. Five steps corresponding to 73% of the gas released give a weighted mean age of 84.2 ± 1.0 Ma. Model

closure temperatures are ~520°C for this amphibole composition assuming a spherical geometry, a grain radius of 80 μm, and a cooling rate of 20°C/m.y. [Dahl, 1996]. Results are interpreted to record cooling below 520°C by ~84 Ma. Biotite from sample 8 also

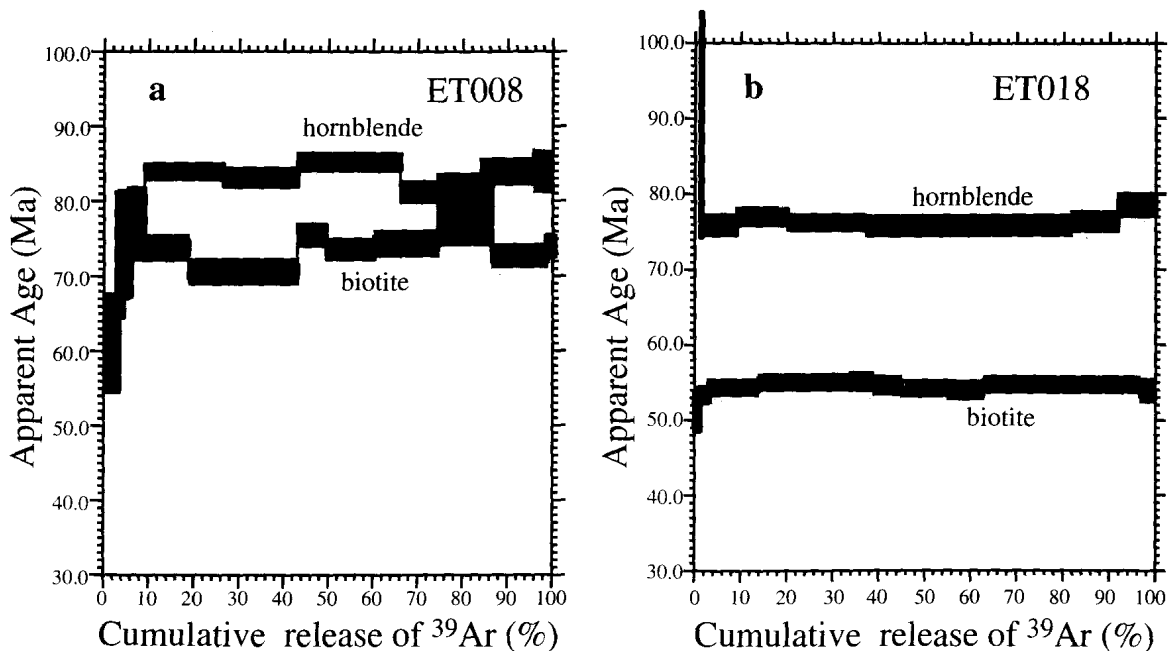


Figure 6. The $^{40}\text{Ar}/^{39}\text{Ar}$ age spectra. (a) Hornblende and biotite samples (sample 8) from paleomagnetic site ET008 on southwestern margin of Ecstall pluton. (b) Hornblende and biotite samples (sample 18) from paleomagnetic site ET018 in central portion of Ecstall pluton. See Table A3 (electronic supplement) and text for explanation.

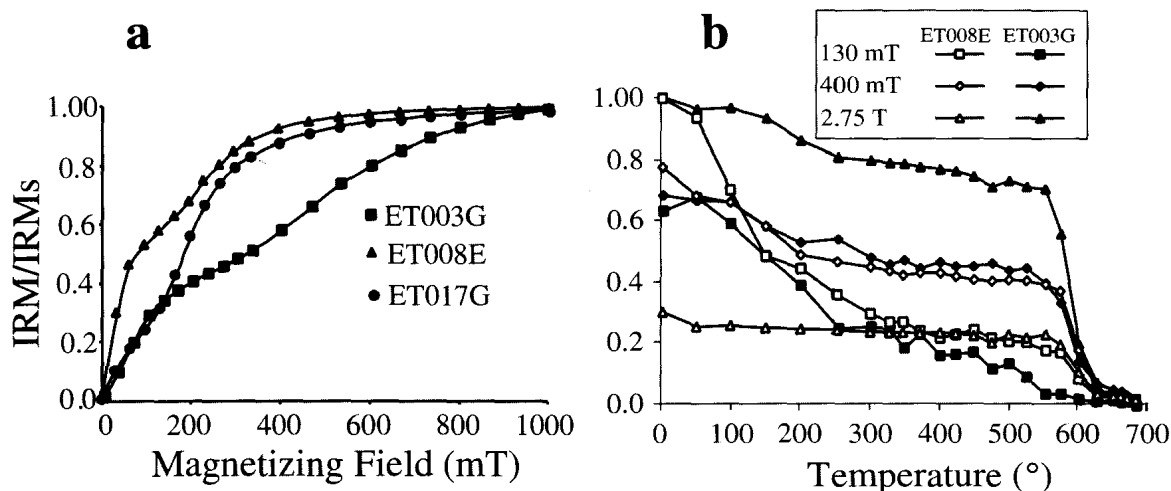


Figure 7. Coercivity spectrum analysis for representative samples from the Ecstall pluton. (a) Normalized acquisition of isothermal remanent magnetism (IRM) versus magnetizing field. (b) Thermal demagnetization of three coercivity fractions versus temperature.

yielded a complex age spectrum but with younger $^{40}\text{Ar}/^{39}\text{Ar}$ apparent ages ranging from 46 to 79 Ma. Six steps corresponding to 59% of the gas released gave a weighted mean age of 73.9 ± 0.6 Ma, which is interpreted to reflect the time at which the sample cooled to below a nominal closure temperature of 300°C [McDougall and Harrison, 1999]. The thermochronologic data for sample 8 indicate that Late Cretaceous crystallization was followed by cooling at rates of $\geq 20^\circ\text{C}/\text{m.y.}$ We infer that the relatively young $^{40}\text{Ar}/^{39}\text{Ar}$ apparent ages associated with the lowest-temperature portion of the age spectra are the result of alteration.

4.2.2. Sample 18. [17] The $^{40}\text{Ar}/^{39}\text{Ar}$ step heat experiments from sample 18 from the central portion of the Ecstall pluton (Figure 4) yielded a flat age spectrum with a plateau age of 76.4 ± 0.6 Ma corresponding to over 98% of the gas released. Model closure temperatures are $\sim 520^\circ\text{C}$ for this composition assuming a spherical geometry, grain radius of $80 \mu\text{m}$, and cooling rate of $20^\circ\text{C}/\text{m.y.}$ [Dahl, 1996]. Results are interpreted to record cooling to below $\sim 520^\circ\text{C}$ by 76 Ma. This sample is relatively unaltered, and no evidence exists for resetting of argon systematics subsequent to this time. Biotite from sample 18 also yielded a flat age spectrum but with a younger $^{40}\text{Ar}/^{39}\text{Ar}$ plateau age of 54.7 ± 0.2 Ma. Biotite results indicate that sample 18 cooled to below a nominal closure temperature of 300°C by early Eocene time. The thermochronologic data for sample 18 indicate Late Cretaceous crystallization followed by Late Cretaceous to early Eocene cooling at rates of $\sim 10^\circ\text{C}/\text{m.y.}$

[18] The geochronologic data indicate that crystallization of the Ecstall pluton at 91 Ma was followed by earlier and more rapid cooling of the western portion (sample 8, Figure 4) compared to the central portion (sample 18, Figure 4) of the pluton. Although our data do not constrain the low-temperature thermal history of the pluton, an apatite fission track age of 38.7 ± 1.9 Ma from the northern end of the Ecstall indicates cooling to below 100°C , and we infer exhumation to shallow levels of the crust by late Eocene time [Harrison et al., 1979].

5. Paleomagnetism

5.1. Procedures and Rock Magnetic Analyses

[19] Collections of paleomagnetic samples were done on the north shore of the Skeena River in road cuts of the Yellowhead Highway or adjacent exposures and along the Canadian National rail line (Figure 2). A dense sample coverage of the northern lobe of the Ecstall pluton was accomplished. Twenty-eight sites were

collected (≥ 8 samples per site) using standard paleomagnetic coring methods. About one third of the samples were oriented by Sun compass and magnetic compass, with the remainder oriented only with magnetic compass. Significant deflections of the magnetic compass were observed within a few meters of the rail line. No samples were collected close to the rail line unless Sun compass orientations could be obtained.

[20] Following preparation, all paleomagnetic samples were stored, measured, and thermally demagnetized in a magnetically shielded room with average field intensity < 200 nT. Measurement of natural remanent magnetism (NRM) was done with a three-axis cryogenic magnetometer (2G Model 755R). Analyses of coercivity spectra of representative samples were performed using the methods of Dunlop [1972] and Lowrie [1990].

[21] Reflected-light microscopy revealed an abundance of highly reflective and anisotropic opaque grains containing fine exsolution structures of a lighter gray mineral. The host grains show no internal reflections. Coupled with rock magnetic analyses described below, these observations suggest that host grains are most likely Ti-poor titanohematite. The lighter gray mineral is probably ilmenite resulting from magmatic exsolution of crystals of intermediate composition titanohematite into composite grains of the dominant Ti-poor titanohematite phase containing finely exsolved Ti-rich ilmenite.

[22] Acquisition of isothermal remanent magnetism (IRM) for most samples from the Ecstall pluton indicates the presence of ferromagnetic minerals with coercive force ≥ 300 mT (Figure 7a). Thermal demagnetization of IRM indicates that the high and intermediate coercivity fractions have unblocking temperatures dominantly between 580°C and 650°C . These IRM data are consistent with the reflected light observations, indicating that Ti-poor titanohematite is the dominant ferromagnetic mineral.

5.2. Anisotropy of Magnetic Susceptibility

[23] Anisotropy of magnetic susceptibility (AMS) was measured using a Sapphire Instruments (model SI-2) magnetic susceptibility bridge. Anisotropy data were generally obtained from six samples per site, and site-mean directions of principal susceptibility axes were determined using bootstrap statistical methods described by Constable and Tauxe [1990]. Only five sites were observed to have AMS greater than 10%. Many sites are isotropic without significant AMS. Because of the low saturation magnetization of Ti-poor titanohematite we infer that AMS is controlled by the fabric of Fe-bearing silicates.

[24] Principal AMS axes from all sites within the Ecstall pluton are shown in Figure 8a. There is much scatter in the directions of principal axes. However, there is a general tendency for minimum susceptibility axes to be subvertical with maximum and intermediate axes being subhorizontal. This indicates a generally flat foliation for the AMS ellipsoids. There is also a less clear tendency for the maximum susceptibility axes to be oriented east-west. A possible interpretation of these AMS patterns is that the Ecstall pluton developed a fabric with subhorizontal foliation and slight east-west lineation as a flow fabric at the time of emplacement.

[25] The eastern portion of the Ecstall pluton has visible fabric increasing in intensity near the eastern margin probably because of proximity to the Coast shear zone (Figure 4). Indeed, the AMS axes observed for the five sites collected from the eastern portion of the Ecstall pluton display within and between site consistency (Figures 8b and 8c). Potential superposition of flow and deformational fabric make interpretation of this AMS complex, and we do not understand this pattern nor its potential relation to the paleomagnetic directions in detail. Nevertheless, we are concerned that the paleomagnetic directions obtained from these eastern sites may have been affected by anisotropy. The paleomagnetic directions from these sites are reported in Table 1 but are not considered further.

5.3. Paleomagnetic Results

[26] The Ecstall pluton is an extraordinary paleomagnetic recorder. For most plutonic rocks the fidelity of the paleomagnetism and the percentage of samples which yield well determined characteristic remanent magnetization (ChRM) directions is limited. The Ecstall pluton provides uncommonly well determined ChRM directions from almost all samples collected.

[27] Thermal demagnetization employed from 8 to 12 temperature steps ranging up to 685°C. The magnetic field inside the thermal demagnetization furnaces was <10 nT. Typical results of thermal demagnetization are illustrated in Figure 9. For most samples, minor components of NRM were unblocked during thermal demagnetization up to 560°C. A characteristic remanent magnetization was isolated from most samples over a narrow unblocking temperature range from ~560°C to ~630°C. The progression of vector end points over four or more successive thermal demagnetization steps in the 560°C to 630°C interval was analyzed using principal component analysis [Kirschvink, 1980] to determine the sample ChRM. ChRM directions for 145 of 162 samples were determined with maximum angular deviation (MAD) <5°, indicating that most sample ChRM directions are precisely determined. Only sample characteristic components determined with MAD ≤20° are considered reliable.

[28] Following determination of sample ChRM directions, site-mean characteristic directions were calculated using standard methods of Fisher [1953]. Only one site failed to yield sufficiently well determined sample ChRM directions to allow determination of a site-mean direction. Most site-mean directions are based on six sample ChRM directions, although two site-mean directions are based on results from four samples. Twenty-three site-mean directions have 95% confidence limits ≤15°. Site-mean ChRM directions are listed in Table 1 and illustrated in Figure 10a. We interpret the ChRM to be a thermal remanent magnetization acquired as these plutonic rocks cooled through the 560°C to 630°C range of blocking temperatures.

6. Discussion

6.1. Distribution of Paleomagnetic Directions

[29] The blocking temperatures of the characteristic magnetization are dominantly in the 580°C to 620°C range. The zircon ages are interpreted to record crystallization, whereas the argon ages record cooling to ~520°C for hornblende and ~300°C for biotite [McDougall and Harrison, 1999]. The ⁴⁰Ar/³⁹Ar horn-

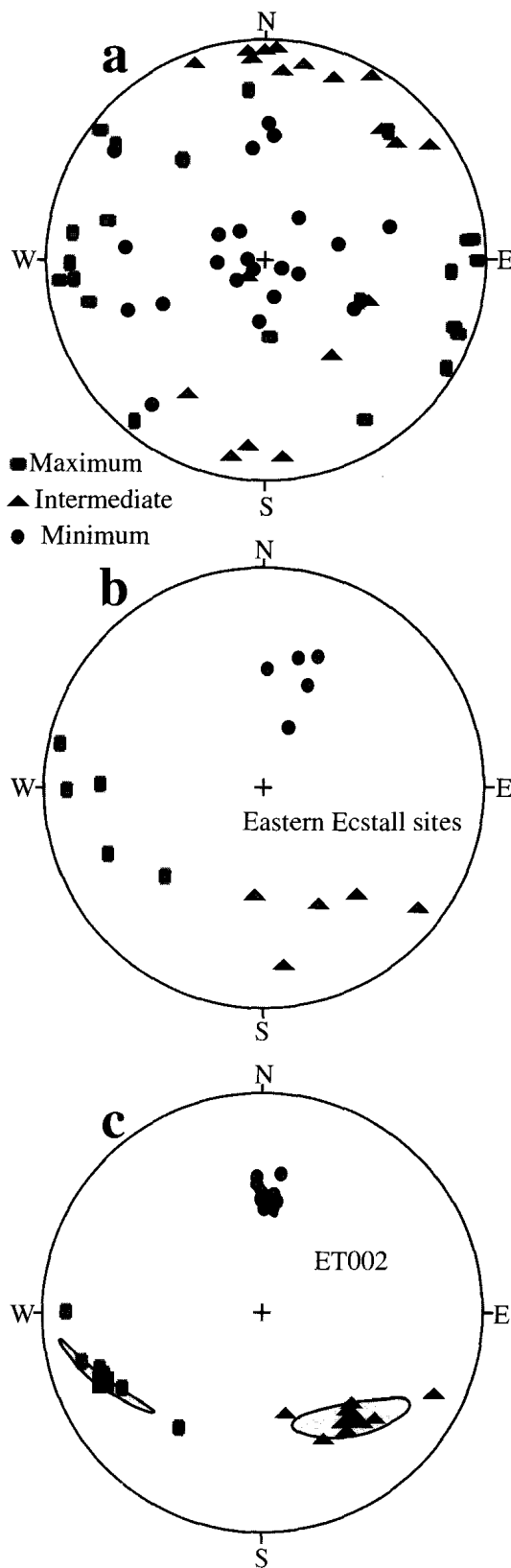


Figure 8. Lower hemisphere equal-area projections of principal axes of anisotropy of magnetic susceptibility (AMS). (a) AMS axes for sites from the western and central portion of the Ecstall pluton. (b) AMS axes for sites from the eastern portion of the Ecstall pluton. (c) Sample AMS axes for site ET002 from the eastern portion of the Ecstall pluton. Mean axes are indicated by the larger symbols enclosed by 95% confidence limits. Axes of maximum susceptibility are shown by squares; axes of intermediate susceptibility are shown by triangles; axes of minimum susceptibility are shown by circles.

Table 1. Site-Mean Characteristic Magnetization Directions^a

Site	Location		Dist, km	N	I, deg	D, deg	J, 10 ⁻¹ A/m	α ₉₅ , deg	k	VGP	
	Lat, °N	Long, °W								Lat, °N	Long, °E
ET001 ^b	54°13.1'	129°54.3'	16.2	6	-65.0	215.6	9.9	3.2	429.7	-66.6	143.2
ET002 ^b	54°13.1'	129°54.8'	15.9	6	-69.2	218.4	9.4	4.9	190.3	-67.4	127.8
ET003 ^b	54°12.9'	129°55.4'	15.0	6	-51.5	263.5	11.0	7.6	78.0	-29.2	124.6
ET004 ^b	54°12.4'	129°56.4'	13.8	5	59.8	67.6	4.3	6.2	154.3	44.2	308.3
ET005 ^b	54°12.4'	129°56.5'	13.7	6	50.0	59.3	3.5	6.4	111.5	42.2	324.4
ET006	54°12.2'	129°57.2'	12.8	5	81.4	17.4	5.0	3.3	545.8	69.7	244.5
ET007	54°9.0'	130°7.3'	0.0	4	11.6	37.7	0.4	20.3	21.6	33.0	3.5
ET008	54°9.1'	130°7.0'	0.4	6	1.5	56.1	1.1	6.7	100.3	19.7	348.0
ET009	54°9.2'	130°6.3'	0.6	6	13.2	53.4	2.3	8.3	66.0	26.2	347.2
ET011	54°9.7'	130°6.0'	2.2	6	-27.6	246.0	8.9	4.8	199.6	-25.8	150.8
ET012	54°10.2'	130°5.3'	3.4	4	23.7	76.4	0.7	20.8	15.4	18.0	323.7
ET013	54°10.4'	130°4.4'	4.5	6	55.3	48.7	1.9	3.7	336.6	52.0	328.4
ET014	54°10.3'	130°3.1'	5.6	4	46.0	65.3	0.8	17.1	29.7	36.2	322.2
ET015	54°10.3'	130°2.7'	5.8	6	-58.5	276.9	1.2	10.8	39.2	-27.2	109.9
ET016	54°10.2'	130°1.6'	6.6	6	-30.8	222.4	1.0	12.6	29.3	-40.2	172.2
ET017	54°10.4'	130°1.2'	7.1	6	-50.6	245.8	1.1	10.7	40.2	-38.8	138.5
ET018	54°12.1'	129°57.3'	12.6	6	80.0	253.6	4.7	8.6	61.5	45.2	203.0
ET019	54°12.1'	129°57.5'	12.5	6	73.6	0.2	7.8	6.4	111.2	84.7	231.4
ET020	54°12.1'	129°57.6'	12.3	6	76.2	343.3	7.7	5.2	169.3	77.1	195.4
ET021	54°12.8'	129°59.3'	11.7	5	-84.1	216.7	9.9	3.7	424.6	-62.8	65.5
ET022	54°13.1'	129°59.6'	11.8	6	-61.0	209.4	6.2	9.2	54.1	-67.1	160.2
ET023	54°13.2'	129°59.7'	11.8	6	-77.8	228.2	11.0	4.8	194.0	-64.1	92.6
ET024	54°13.8'	130°1.8'	10.7	6	77.2	69.5	5.0	6.5	106.3	55.5	273.0
ET025	54°13.9'	130°1.7'	10.8	6	72.3	30.5	0.8	10.5	41.6	72.7	297.0
ET026	54°14.1'	130°1.8'	10.8	5	73.3	357.1	5.1	15.9	24.2	85.0	212.7
ET027	54°14.3'	130°2.0'	10.9	6	73.8	105.2	5.1	11.6	34.2	38.7	268.3
ET028	54°14.3'	130°2.8'	10.4	6	-61.4	252.2	4.3	4.1	269.2	-42.9	123.1

^a Site, number for paleomagnetic site; Location, site location; Lat, latitude; Long, longitude; Dist, distance of site from southwest margin of Ecstall pluton; N, number of samples used to determine site-mean direction; I and D, inclination and declination of site-mean direction; J, geometric mean intensity of characteristic remanent magnetization component; α₉₅, radius of cone of 95% confidence about site-mean direction; k, concentration parameter; VGP, site-mean virtual geomagnetic pole computed from the site-mean direction.

^b Sites with significant and consistent anisotropy of magnetic susceptibility. These site-mean directions are not used in structural interpretations.

blende ages closely approximate the age for acquisition of the characteristic magnetization. These ages are ~84 Ma for the southwestern margin and ~76 Ma for the central portion of the pluton. Following the Cretaceous normal-polarity superchron, geomagnetic reversals commenced at ~83 Ma according to the geomagnetic polarity timescale of *Cande and Kent* [1992, 1995].

Polarities of ChRM are shown on the sample location map (Figure 4). Sites on the west and north sides are dominated by normal polarity. Proceeding toward the interior of the pluton, a reversed polarity zone is observed surrounding the normal-polarity zone at the center of the northern lobe of the Ecstall pluton. With cooling and magnetization proceeding from the margin inward, the

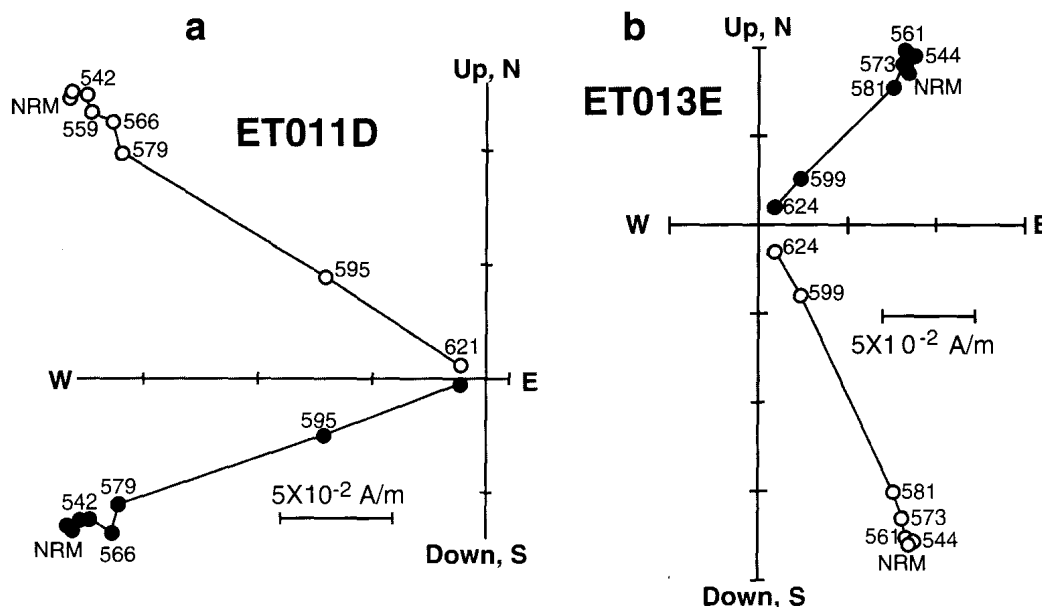


Figure 9. Vector component diagrams of thermal demagnetization behavior. Open circles are projections onto vertical plane, and solid circles are projections onto horizontal plane. Numbers adjacent to data points indicate temperature (in °C).

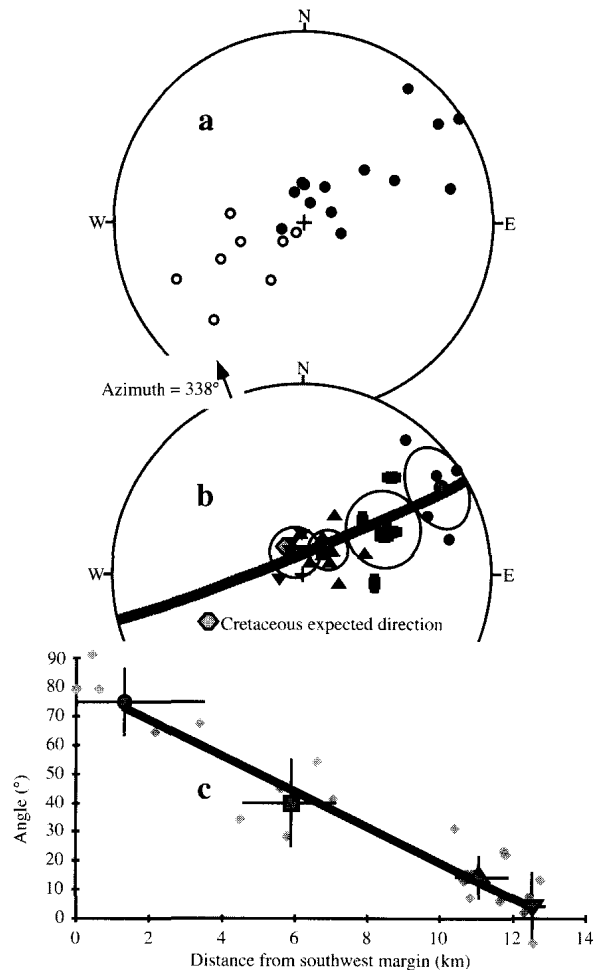


Figure 10. (a) Equal-area projection of site-mean ChRM directions. Solid circles indicate directions in lower hemisphere of projection, and open circles indicate directions in upper hemisphere. (b) Site-mean directions grouped by distance of sampling site from southwestern margin of the Ecstall pluton. Site-mean directions from reverse polarity sites have been inverted through the origin. Directions from sites within 3.4 km from southwestern margin are shown by circles; directions from sites 3.4 to 7.1 km from southwestern margin are shown by squares; directions from sites 10.4 to 11.8 km from southwestern margin are shown by triangles; directions from sites 12.3 to 12.8 km from southwestern margin are shown by inverted triangles. Mean directions for groups of sites are indicated by larger shaded symbols along with 95% confidence limits. Light shaded hexagon is the expected Late Cretaceous magnetic field direction at the sampling location. Shaded arc is small circle with axis at azimuth 338° . (c) Angular distance of site-mean directions (shaded diamonds) and group-mean directions (larger symbols corresponding to those in Figure 10b) from the expected Late Cretaceous direction measured along the small circle versus distance of sampling sites from southwestern margin of the Ecstall pluton. Vertical lines through group-mean directions are 95% confidence limits, while horizontal lines indicate the range of distance of sampling sites from the southwestern margin of the pluton.

outer normal-polarity sites were likely magnetized during the final stages of the Cretaceous normal-polarity superchron. The zone of reversed polarity sites surrounding the central portion of the pluton was magnetized during chron 33r, while the central normal-polarity sites were magnetized during chron 33.

[30] As shown in Figure 10a, site-mean ChRM directions have a streaked distribution. Three observations indicate that streaking is

not due to mixture of multiple components or different polarities of magnetization.

1. Mixing of components of magnetization often leads to multiple linear segments or curved trajectories on vector component diagrams because of differences in unblocking temperatures between components [Dunlop, 1979]. Instead, sample ChRM directions from the Ecstall pluton are defined by single linear trajectories of vector end points with no indication of curvature (Figure 9).

2. Recording of a polarity transition would likely produce streaking of sample ChRM directions within sites of the transition zone because of differences in blocking temperatures between samples. We observe no such within-site streaking of directions.

3. The divergent site-mean directions within a polarity transition zone would be confined to a region of the pluton separating zones of normal and reversed polarities. Instead, we observe sharply defined polarity boundaries with adjacent sites having antipodal directions (Figure 4).

[31] The streaked distribution of site-mean ChRM directions is related to location of the sampling site along the southwest to northeast transect across the Ecstall pluton. Four groups of paleomagnetic sites with four to eight sites each were formed according to distance of site from the southwestern margin of the pluton (Table 1 and Figure 4). Individual site-mean directions and the group-mean directions are shown in Figure 10b, with all directions converted to normal polarity. Group-mean directions are listed in Table 2. Also shown on Figure 10b is the expected Cretaceous magnetic field direction ($I = 78.0^\circ \pm 2.1^\circ$; $D = 331.1^\circ \pm 9.5^\circ$ [Van Fossen and Kent, 1992]) at the present location of the Ecstall pluton. The group-mean directions are distributed along a small circle with axis at 338° azimuth. The group-mean direction for sites farthest from the southwestern margin (most central site locations surrounding the site with $^{40}\text{Ar}/^{39}\text{Ar}$ hornblende age of 76 Ma) is concordant with the expected Cretaceous direction. Groups closer to the southwestern margin of the pluton have mean directions progressively divergent from this expected direction. The angles along the small circle between group-mean directions and the expected Cretaceous direction are plotted in Figure 10c. The regression line shows a regular decrease in angle with distance of sampling sites from the southwestern margin where the $^{40}\text{Ar}/^{39}\text{Ar}$ hornblende age of 84 Ma was obtained.

6.2. Latitudinal Transport During Magnetization?

[32] The paleomagnetic directions observed from sites near the southwestern margin of the Ecstall pluton have shallow inclinations and clockwise declinations compared to the expected Cretaceous direction. In the Baja British Columbia model, northward transport accounts for the observed shallow paleomagnetic inclination, while clockwise vertical axis rotation of terranes during transport accounts for the discordant declination [Beck, 1980; Irving et al., 1996]. An obvious hypothesis to test is whether the progressive discordance of paleomagnetic directions with position

Table 2. Group-Mean Directions^a

Average Distance, km	<i>N</i>	<i>I</i> , deg	<i>D</i> , deg	α_{95} , deg	Angle, deg
1.3	5	15.9	57.5	16.6	75
5.9	5	49.7	61.3	16.4	40
11.1	8	74.9	48.7	8.5	14
12.5	4	80.8	342.6	11.3	4

^a Average distance of group of sites from southwestern margin of Ecstall pluton; *N*, number of sites in group; *I* and *D*, inclination and declination of group-mean direction; α_{95} , radius of cone of 95% confidence about group-mean direction; Angle, small-circle angle of group mean from expected Cretaceous direction.

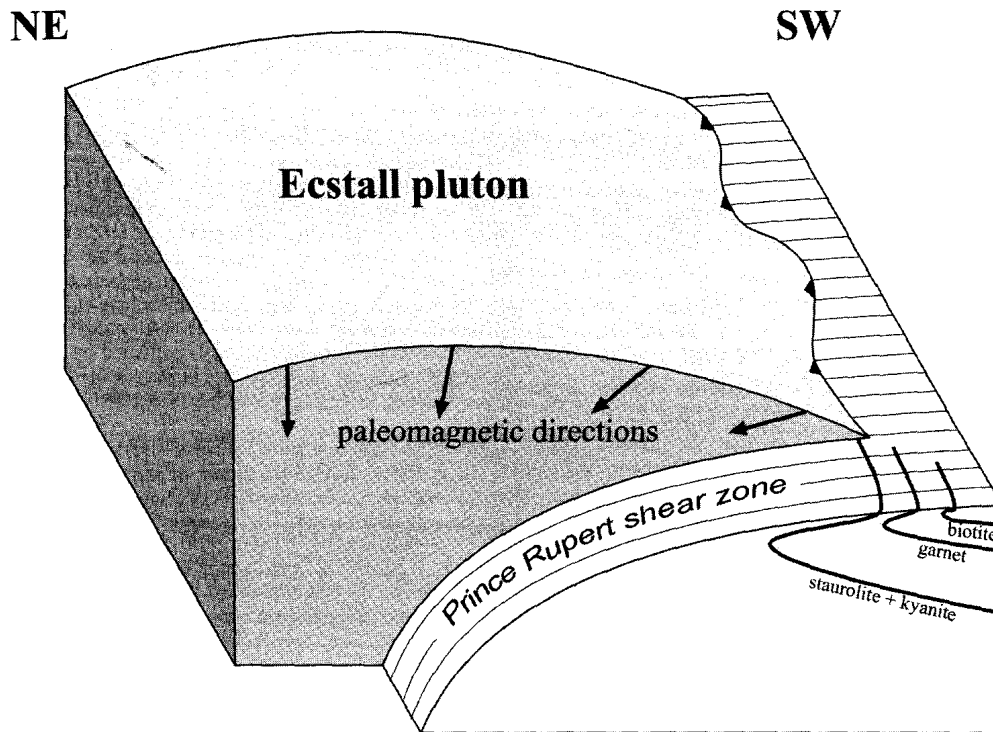


Figure 11. Folding model. Ecstall pluton is shown above west vergent and convex upward Prince Rupert Shear Zone. Metamorphic isograds mapped west of Prince Rupert Shear Zone are illustrated by heavy lines. Arrows indicate paleomagnetic directions, which are distributed along small circle centered on the fold axis. View is toward south.

in the Ecstall pluton could be explained by tectonic transport during cooling and magnetization.

[33] Two difficulties faced by the tectonic transport hypothesis are the magnitude of motion required and the rate at which that motion must have occurred. The group-mean direction for sites closest to the southwestern margin of the Ecstall pluton is discordant from the expected Cretaceous direction by $>70^\circ$ (Figure 10). The observed inclination is $>60^\circ$ shallower than the expected direction. To account for this inclination shallowing by latitudinal transport requires ~ 7000 km of transport since the magnetization was acquired at 84 Ma. Interior portions of the Ecstall pluton have concordant paleomagnetic directions, indicating little or no latitudinal transport since magnetization at 76 Ma. Thus the tectonic transport hypothesis requires 7000 km of latitudinal motion to have occurred during the ~ 8 m.y. interval over which the Ecstall pluton acquired its magnetization. The implied transport rate of ~ 900 km/m.y. (≈ 1 m/yr) exceeds plausible lithospheric plate velocities by an order of magnitude. An explanation of the Ecstall pluton paleomagnetism in terms of tectonic transport alone must be abandoned.

6.3. Tilting During Magnetization?

[34] Northeast-side-up tilting of the Ecstall pluton during uplift can produce the highly discordant paleomagnetic directions on the southwestern margin of the pluton along with concordant directions in the pluton interior. A model of synchronous tilting and magnetization was developed by Beck [1992]. For northeast-side-up tilt, portions of a pluton progressively uplift through the magnetic blocking temperature isotherm producing a small-circle distribution of paleomagnetic directions and a decrease of cooling ages toward the northeast. The axis of the resulting small-circle distribution of paleomagnetic directions is the axis to tilting. Sites on the southwestern margin acquire magnetization first and experience maximum tilting since magnetization. To account for the observed paleomagnetic directions within the Ecstall pluton, the amount of tilt required since magnetization of these south-

western sites is $>70^\circ$. Sites toward the pluton interior become magnetized at progressively later times and record smaller amounts of tilt. However, this coherent tilt model encounters a major problem when the geobarometric data from the Ecstall pluton are considered.

[35] With a southwest to northeast dimension of ~ 20 km for the Ecstall pluton (Figure 4) a rigid 70° northeast-side-up tilt implies a structural relief of >15 km across the pluton. In turn, this would require a systematic increase of ~ 400 MPa in geobarometric pressure from southwest to northeast across the pluton. However, the geobarometric data presented above indicate that pressures during crystallization of hornblende were in the 740–830 MPa (7.4–8.3 kbar) range across the full width of the pluton. Thus the pressure increase predicted by the coherent tilt model is contradicted by the geobarometric data. Moreover, explaining a coherent 70° tilt of a crustal block the size of the Ecstall pluton presents a major structural geologic challenge.

6.4. Folding of the Western Margin

[36] Because the axis of the small-circle distribution of paleomagnetic directions is aligned with major structures in the Prince Rupert region, an explanation involving local deformation is suggested. Viable explanations are constrained by the geobarometric data to require only modest (<5 km) structural relief across the Ecstall pluton. Because pressures of equilibration for metamorphic assemblages in the country rocks and pressures of crystallization within the pluton indicate depths of ~ 25 km, only models implying modest structural relief between the country rocks and the pluton are realistic. Our preferred interpretation of the paleomagnetic, geochronologic, and geobarometric data from the Ecstall pluton involves folding of the western margin of the pluton into a west vergent anticline (Figure 11).

[37] A local folding of the southwestern margin of the Ecstall pluton (Figure 11) is consistent with available data. From patterns of metamorphic grade and fabrics, Crawford *et al.* [1987] interpret

the Prince Rupert Shear Zone as a Late Cretaceous west directed thrust with the Ecstall pluton in the upper plate. Crawford *et al.* [1987] further suggest that intrusion of the Ecstall pluton at an intermediate to deep crustal level may have facilitated motion on west vergent thrust faults in this region. The southwest margin of the Ecstall pluton has a NNW-SSE orientation as does the Prince Rupert Shear Zone as it passes west of the pluton (Figure 4). This orientation is in agreement with the $\sim 340^\circ$ azimuth of the small-circle distribution of paleomagnetic directions (Figure 10).

[38] From patterns of metamorphic grade and fabric observations, a convex upward geometry has been proposed for thrust faults within the Western Metamorphic Belt including the Prince Rupert Shear Zone [Crawford *et al.*, 1987; Chardon *et al.*, 1999]. The structural relations between the Ecstall pluton and the underlying Prince Rupert Shear Zone (Figure 11) suggest two possible scenarios for folding. One possibility is that the Prince Rupert shear was originally planar at the present level of exposure and that both the shear zone and the overlying Ecstall pluton were folded after thrusting had ceased. A second possibility is that the Prince Rupert Shear Zone was originally convex upward at the level of exposure and that hanging wall rocks (including the Ecstall pluton) were folded as they moved over this segment of the fault. In essence, this second model is a large fault-bend fold. Either model can produce the small-circle distribution of paleomagnetic directions with highly discordant directions on the western margin and concordant directions in the pluton interior. Both models are consistent with the geobarometric data because they require only modest structural relief between the pluton and the country rocks. Both models are also consistent with existing geochronologic, thermochronologic, and structural data from the region. At this time, available data do not clearly favor one model over the other.

7. Conclusions

[39] Crystallization of the Ecstall pluton took place during a short interval at ~ 90 Ma. Geobarometric data indicate that the portion of the pluton now exposed at the present erosion surface crystallized at ~ 25 to ~ 30 km depth. Acquisition of magnetization took place by cooling to $\sim 580^\circ\text{C}$ and was soon followed by cooling to $\sim 520^\circ\text{C}$ required for retention of argon in hornblende at 84 Ma for the western margin and at 76 Ma for the central portion of the pluton. Cooling to below 300°C was not complete until 74 Ma for the western margin and 55 Ma for the center of the pluton. Paleomagnetic directions from sites within 4 km of the western margin of the Ecstall pluton are deflected $\sim 70^\circ$ from the expected Cretaceous magnetic field direction, while sites from the pluton interior yield concordant directions. The distribution of paleomagnetic directions is along a small circle with subhorizontal axis at $\sim 340^\circ$ azimuth. The paleomagnetic observations are compatible with northward transport of 500 km to perhaps 1000 km as suggested by some geologic analyses [Price and Charni-chael, 1986]. However, explanation of the paleomagnetic directions entirely by northward transport (Baja British Columbia hypothesis) during the ~ 84 Ma to 76 Ma interval of magnetization requires latitudinal motion at a rate exceeding lithospheric plate velocities by a factor of 10. Coherent 70° northeast-side-up tilt during cooling and magnetization could produce the patterns of $^{40}\text{Ar}/^{39}\text{Ar}$ ages and the paleomagnetic directions but is contradicted by the geobarometric data. Local folding of the Ecstall pluton can account for the geochronologic, paleomagnetic, and geobarometric data and is supported by mapped structural geology of the Prince Rupert area. This folding could have resulted either from Late Cretaceous thrust displacement of the Ecstall pluton above the convex upward Prince Rupert Shear Zone or later folding of both the pluton and the underlying shear zone.

which were part of the Continental Dynamics ACCRETE Project with Principal Investigators Lincoln Hollister and Maria Luisa Crawford. Field assistance was provided by Brigitte Martini and Brian LaReau. The logistical support and local expertise provided by Peter Freeman and Ron Payne were much appreciated. Carol Evenchick provided contacts with Canadian National Rails officials who in turn provided logistical assistance. Paleomagnetic laboratory technical assistance was provided by Bill Hart, Orestes Morfin, and Hillary Brown. We are grateful to Bin Li for assistance in the Noble Gas Laboratory. This project benefited from expert computer systems management and programming by Steve Sorenson. We thank Chris Eastoe for expert assistance with polished section analysis. Thoughtful comments by reviewers Ken Kodama, Bernie Housen, and Associate Editor Steve Lund led to improvements in the manuscript. Discussions with Lincoln Hollister and Maria Luisa Crawford provided insight into constraints on deformational models provided by metamorphic petrology and structural geology of areas surrounding the Ecstall pluton.

References

- Ague, J. J., and M. T. Brandon, Regional tilt of the Mt. Stewart batholith, Washington, determined using aluminum in hornblende barometry: Implications for northward translation of Baja British Columbia, *Geol. Soc. Am. Bull.*, 108, 471–488, 1996.
- Ague, J. J., and M. T. Brandon, Regional tilt of the Mount Stuart batholith, Washington, determined using aluminum-in-hornblende barometry: Implications for northward translation of Baja British Columbia: Discussion, *Geol. Soc. Am. Bull.*, 109, 1225–1227, 1997.
- Anderson, J. L., Regional tilt of the Mount Stuart batholith, Washington, determined using aluminum-in-hornblende barometry: Implications for northward translation of Baja British Columbia: Discussion, *Geol. Soc. Am. Bull.*, 109, 1223–1225, 1997.
- Armstrong, R. L., and D. Runkle, Rb-Sr geochronometry of the Ecstall, Kitkiata, and Quottoon plutons and their country rocks, Prince Rupert region, Coast Plutonic complex, British Columbia, *Can. J. Earth Sci.*, 16, 387–399, 1979.
- Beck, M. E. Jr., Discordant paleomagnetic pole position as evidence of regional shear in the western Cordillera of North America, *Am. J. Sci.*, 276, 694–712, 1976.
- Beck, M. E., Paleomagnetic record of plate-margin tectonics processes along the western edge of North America, *J. Geophys. Res.*, 85, 7115–7131, 1980.
- Beck, M. E. Jr., Some thermal and paleomagnetic consequences of tilting a batholith, *Tectonics*, 11, 297–302, 1992.
- Beck, M. E. Jr., R. F. Burmester, and R. Schoonover, Paleomagnetism and tectonics of Cretaceous Mt. Stuart batholith of Washington: Translation or tilt?, *Earth Planet. Sci. Lett.*, 56, 336–342, 1981.
- Brown, E. H., and R. F. Burmester, Metamorphic evidence for tilt of the Spuzzum pluton: Diminished basis for the “Baja British Columbia” concept, *Tectonics*, 10, 978–985, 1991.
- Butler, R. F., G. E. Gehrels, W. C. McClelland, S. R. May, and D. Klepacki, Discordant paleomagnetic poles from the Canadian Coast Plutonic Complex: Regional tilt rather than large-scale displacement?, *Geology*, 17, 691–694, 1989.
- Cande, S. C., and D. V. Kent, A new geomagnetic polarity time scale for the Late Cretaceous and Cenozoic, *J. Geophys. Res.*, 97, 13,917–13,951, 1992.
- Cande, S. C., and D. V. Kent, Revised calibration of the geomagnetic polarity timescale for the Late Cretaceous and Cenozoic, *J. Geophys. Res.*, 100, 6093–6095, 1995.
- Chardon, D., C. L. Andronicos, and L. S. Hollister, Large-scale transpressive shear zone patterns and displacements within magmatic arcs: The Coast Plutonic Complex, British Columbia, *Tectonics*, 18, 278–292, 1999.
- Constable, C., and L. Tauxe, The bootstrap for magnetic susceptibility tensors, *J. Geophys. Res.*, 95, 8383–8395, 1990.
- Cowan, D. S., Alternative hypotheses for the mid-Cretaceous paleogeography of the Western Cordillera, *GSA Today*, 4, 181–186, 1994.
- Cowan, D. S., M. T. Brandon, and J. L. Garver, Geologic tests of hypotheses for large coastwise displacements—A critique illustrated by the Baja British Columbia controversy, *Am. J. Sci.*, 297, 117–173, 1997.
- Crawford, M. L., and L. S. Hollister, Contrast of metamorphic and structural histories across the Work Channel lineament, Coast Plutonic Complex, British Columbia, *J. Geophys. Res.*, 87, 3849–3860, 1982.
- Crawford, M. L., L. S. Hollister, and G. J. Woodsworth, Crustal deformation and regional metamorphism across a terrane boundary, Coast Plutonic Complex, British Columbia, *Tectonics*, 6, 343–361, 1987.
- Crawford, M. L., W. A. Crawford, and G. E. Gehrels, Terrane assembly and structural relationships in the eastern Prince Rupert quadrangle, British Columbia, in *Tectonics of the Coast Mountains in Southeast Alaska and Coastal British Columbia*, edited by H. H. Stowell and W. C. McClelland, *Spec. Pap. Geol. Soc. Am.*, 343, 1–21, 2000.

[40] **Acknowledgments.** This research was funded by National Science Foundation grants EAR-9526334, EAR-9526263, and EAR-9526334,

- Dahl, P. S., The effects of composition on retentivity of argon and oxygen in hornblende and related amphiboles: A field-tested empirical model, *Geochim. Cosmochim. Acta*, *60*, 3687–3700, 1996.
- Dunlop, D. J., Magnetic mineralogy of unheated and heated red sediments by coercivity spectrum analysis, *Geophys. J. R. Astron. Soc.*, *27*, 37–55, 1972.
- Dunlop, D. J., On the use of Zijdeveld vector diagrams in multicomponent paleomagnetic samples, *Phys. Earth Planet. Sci. Lett.*, *20*, 12–24, 1979.
- Fisher, R. A., Dispersion on a sphere, *Proc. R. Soc. London, Ser. A*, *217*, 295–305, 1953.
- Gehrels, G. E., Introduction to detrital zircon studies of Paleozoic and Triassic strata in western Nevada and northern California, in *Paleozoic and Triassic Paleogeography and Tectonics of Western Nevada and Northern California*, edited by M. J. Soreghan and G. E. Gehrels, *Spec. Pap. Geol. Soc. Am.*, *347*, 1–17, 2000.
- Gehrels, G. E., Geology and U-Pb geochronology of the Chatham Sound area, southeast Alaska and coastal British Columbia, *Can. J. Earth Sci.*, in press, 2001.
- Gehrels, G. E., and P. A. Kapp, Detrital geochronology and regional correlation of metasedimentary rocks in the Coast Mountains, southeastern Alaska, *Can. J. Earth Sci.*, *35*, 269–279, 1998.
- Hammerstrom, J. M., and E.-A. Zen, Aluminium in hornblende: An empirical igneous geobarometer, *Am. Mineral.*, *71*, 1297–1313, 1986.
- Harrison, T. M., R. L. Armstrong, C. W. Naeser, and J. E. Harakal, Geochronology and thermal history of the Coast Plutonic Complex, near Prince Rupert, British Columbia, *Can. J. Earth Sci.*, *16*, 400–410, 1979.
- Hollister, L. S., and C. L. Andronicos, A candidate for the Baja British Columbia Fault System in the Coast Plutonic Complex, *GSA Today*, *7*, 1–7, 1997.
- Hutchison, W. W., Geology of the Prince Rupert-Skeena map area, British Columbia, *Mem. Geol. Surv. Can.*, *394*, 116 pp., 1982.
- Irving, E., G. J. Woodsworth, P. J. Wynne, and A. Morrison, Paleomagnetic evidence for displacement of the south of the Coast Plutonic Complex, British Columbia, *Can. J. Earth Sci.*, *22*, 584–598, 1985.
- Irving, E., P. J. Wynne, D. J. Thorkelson, and P. Schiarizza, Large (1000 to 4000 km) northward movements of tectonic domains in the northern Cordillera, 83 to 45 Ma, *J. Geophys. Res.*, *101*, 17,901–17,916, 1996.
- Kirschvink, J. L., The least-squares line and plane and the analysis of paleomagnetic data, *Geophys. J. R. Astron. Soc.*, *62*, 699–718, 1980.
- Leake, B. E., Nomenclature of amphiboles, *Mineral. Mag.*, *42*, 533–563, 1978.
- Lowrie, W., Identification of ferromagnetic minerals in a rock by coercivity and unblocking temperature properties, *Geophys. Res. Lett.*, *17*, 159–162, 1990.
- Ludwig, K. R., A computer program for processing Pb-U-Th isotopic data, *U.S. Geol. Surv. Open File Rep.*, *88-542*, 1991a.
- Ludwig, K. R., A plotting and regression program for radiogenic-isotopic data, *U.S. Geol. Surv. Open File Rep.*, *91-445*, 1991b.
- Mahoney, J. B., B. Tikoff, J. Maxson, and R. A. Haugerud, Terrane accretion along the western cordilleran margin: Constraints on timing and displacement, *GSA Today*, *10*, 11–13, 2000.
- McDougall, I., and T. M. Harrison, *Geochronology and Thermochronology by the $^{40}\text{Ar}/^{39}\text{Ar}$ Method*, 2nd ed., 269 pp., Oxford Univ. Press, New York, 1999.
- Price, R. A., and D. M. Charmichael, Geometric test for Late Cretaceous-Paleocene intracontinental transform faulting in the Canadian Cordillera, *Geology*, *14*, 468–471, 1986.
- Schmidt, M., Amphibole composition in tonalite as a function of pressure: An experimental calibration of the Al-in-hornblende barometer, *Contrib. Mineral. Petrol.*, *110*, 304–310, 1992.
- Steiger, R. H., and E. Jäger, Subcommittee on geochronology: Convention on the use of decay constants in geo- and cosmochronology, *Earth Planet. Sci. Lett.*, *36*, 359–362, 1977.
- Symons, D. T. A., Age and tectonic implications of paleomagnetic results from plutons near Prince Rupert, British Columbia, *J. Geophys. Res.*, *79*, 2690–2697, 1974.
- Symons, D. T. A., Paleomagnetism of Mesozoic plutons in the westernmost Coast Complex of British Columbia, *Can. J. Earth Sci.*, *14*, 2127–2139, 1977.
- Umhoefer, P. J., Northward translation of “Baja British Columbia” along the Late Cretaceous to Paleocene margin of western North America, *Tectonics*, *6*, 377–394, 1987.
- Vandall, T. A., Cretaceous Coast Belt paleomagnetic data from the Spetch Creek pluton, B.C.: Evidence for the “tilt and moderate displacement” model, *Can. J. Earth Sci.*, *30*, 1037–1048, 1993.
- Van Fossen, M. C., and D. V. Kent, Paleomagnetism of 122 Ma plutons in New England and the mid-Cretaceous paleomagnetic field in North America: True polar wander or large-scale differential mantle motion?, *J. Geophys. Res.*, *97*, 19,651–19,661, 1992.
- Ward, P. D., J. M. Hurtado, J. L. Kirschvink, and K. L. Verosub, Measurements of the Cretaceous paleolatitude of Vancouver Island: Consistent with the Baja-British Columbia hypothesis, *Science*, *277*, 1642–1645, 1997.
- Woodsworth, G. J., W. D. Loveridge, R. R. Parrish, and R. W. Sullivan, Uranium-lead dates from the Central Gneiss Complex and Ecstall pluton, Prince Rupert map area, British Columbia, *Can. J. Earth Sci.*, *20*, 1475–1483, 1983.
- Wynne, P. J., E. Irving, J. A. Maxson, and K. L. Kleinspehn, Paleomagnetism of the Upper Cretaceous strata of Mount Tatlow: Evidence for 3000 km of northward displacement of the eastern Coast Belt, British Columbia, *J. Geophys. Res.*, *100*, 6073–6091, 1995.
- Zen, E., and J. M. Hammerstrom, Magmatic epidote and its petrologic significance, *Geology*, *12*, 515–518, 1984.

S. Baldwin, Department of Earth Sciences, Syracuse University, Syracuse, NY 13244-1070, USA. (sbaldwin@syr.edu)

R. F. Butler and G. E. Gehrels, Department of Geosciences, University of Arizona, Tucson, AZ 85721-0077, USA. (butler@geo.arizona.edu; ggehrels@geo.arizona.edu)

C. Davidson, Department of Geology, Beloit College, Beloit, WI 53511, USA. (davidson@beloit.edu)